

# Preparation and characterization of long-circulating PELMD/mPEG–PLGA-mixed micelles for 10-hydroxycamptothecin

Shaoping Yin · Juan Li · Nannan Li ·  
Guangji Wang · Xiaochen Gu

Received: 10 September 2013 / Accepted: 13 January 2014  
© Springer Science+Business Media Dordrecht 2014

**Abstract** A novel long-circulating nano-delivery system was constructed using block copolymers of poly monomethoxy-(ethylene glycol)-poly(D,L-lactic-co-glycolic acid)-poly(3(S)-methyl-morpholine-2,5-dione) (PELMD) and poly-monomethoxy (ethylene glycol)-poly-(D,L-lactic-co-glycolic acid) (mPEG–PLGA). The two copolymers possessed satisfactory critical micelle concentration and hemolytic effect. Antitumor compound 10-hydroxycamptothecin (HCPT) was loaded to the mixed micelles to further characterize in vitro and in vivo properties. HCPT-mixed micelles were measured 165–205 nm in particle size, with spherical core–shell structure and uniform-size distribution. The zeta potentials of the mixed micelles ranged 15–20 mV, attributed to the polydesipeptide. Stability of the mixed micelles was improved without complex synthesis. Drug release from the mixed micelles was pH-dependent, which

was beneficial for improving specific drug targeting to tumor tissues. HCPT-mixed micelles demonstrated prolonged retention and tissue targeting in animal models. Mean residence time ( $MRT_{0 \rightarrow \infty}$ ) of HCPT-mixed micelles was significantly longer than that of HCPT injection, and biodistribution of the mixed micelles showed specific drug disposition in liver and lungs. The results indicated that PELMD/mPEG–PLGA-mixed micelles could become a potential drug delivery system for anticancer drugs to improve therapeutic efficacy and minimize adverse effects.

**Keywords** Amphiphilic block copolymers · Mixed micelles · Specific drug targeting · Pharmacokinetics and distribution · Cancer chemotherapy · Nanomedicine

## Introduction

Cancer is one of the most common and significant health threats to humans, and the rate of new cancers diagnosed annually is rapidly increasing worldwide. Chemotherapy is a primary treatment of choice for cancer patients. However, there are numerous technical challenges to an efficient and safe chemotherapy, due to unique anatomy and physiology of tumor development, such as quick proliferation, metastasis, and difficulty in site-targeting drug delivery (Chen and Debnath 2010). A majority of chemotherapy agents are factually cytotoxic compounds lack of therapeutic

S. Yin · J. Li (✉) · N. Li  
Department of Pharmaceutics, State Key Laboratory of Natural Medicines, China Pharmaceutical University,  
24 Tong Jia Xiang, Nanjing 210009, China  
e-mail: lijuancpu@163.com

G. Wang  
Center of Pharmacokinetics, Key Laboratory of Drug Metabolism and Pharmacokinetics, China Pharmaceutical University, 24 Tong Jia Xiang, Nanjing 210009, China

X. Gu  
Faculty of Pharmacy, University of Manitoba, 750  
McDermot Avenue, Winnipeg, MB R3E 0T5, Canada

discriminability; they kill both malignant neoplasm and normal cells/tissues (Han et al. 2007; Niu et al. 2012). Developing a specific drug delivery system with maximal cytotoxicity to tumors yet minimal toxicity to normal tissues has always been an important and critical field in cancer research.

Biodegradable polymeric micelles have become a promising tool for efficient chemotherapy lately; extensive investigations have been focused on formulating and testing nanoparticles made of block, graft, and supermolecular biodegradable polymers (Pan et al. 2007; Lo et al. 2010; Zelinsky and May 2011). Poly(lactide-*co*-glycolic acid) (PLGA) is one of the most common materials for nano drug delivery systems because of satisfactory biocompatibility and biodegradability (Esmaeili et al. 2008). Nevertheless, PLGA nanoparticles are eliminated rapidly from systemic circulation *in vivo*; as a result, PEG-PLGA has been extensively studied in order to improve drug circulation time and tumor targeting (Gryparis et al. 2007; Fernández-Carballido et al. 2008; Chen et al. 2011). Micelles composed of a PEG shell have demonstrated capability of increasing circulation time (Moghimani et al. 2001; Alexis et al. 2008), which would prolong exposure of anticancer drugs to tumor cells and facilitate passive drug targeting through enhanced permeability and retention (EPR) effect (Maeda et al. 2000). Nevertheless, PEGs often encounter particle aggregation *in vitro* and elimination increment by mononuclear phagocytic systems (MPS) *in vivo*, which compromise their formulation stability and therapeutic feasibility. Numerous biodegradable polydepsipeptides have been utilized to stabilize micelles (Chen et al. 2006); among them was a new triblock copolymer poly(ethylene glycol)-poly(L-lactide)-poly(3(*S*)-methyl-morpholine-2,5-dione) (Zhao et al. 2012).

In this study, we prepared long-circulating PELMD/mPEG-PLGA-mixed micelles in an aqueous medium on the basis of a novel biodegradable polymer poly-monomethoxy-(ethylene glycol)-poly(D,L-lactic-*co*-glycolic acid)-poly(3(*S*)-methyl-morpholine-2,5-dione) (PELMD). Anticancer compound 10-hydroxy-camptothecin (HCPT) was then incorporated in the mixed micelles to further characterize *in vitro* and *in vivo* properties of the prepared drug carrier system. As shown in Scheme 1, it was hypothesized that HCPT-mixed micelles would accumulate in tumor tissues by means of passive targeting

or EPR effect, and that cellular uptake of HCPT-mixed micelles would be increased through electrostatic attraction between the positively charged HCPT-mixed micelles and the negatively charged tumor cell membrane. Once inside the tumor cells, HCPT-mixed micelles would achieve endosome/lysosome escape, hence improving intracellular drug release and increasing antitumor efficiency. The ultimate objective of the study was to develop a feasible copolymer-based nano-carrier system for anticancer compounds.

## Experimental section

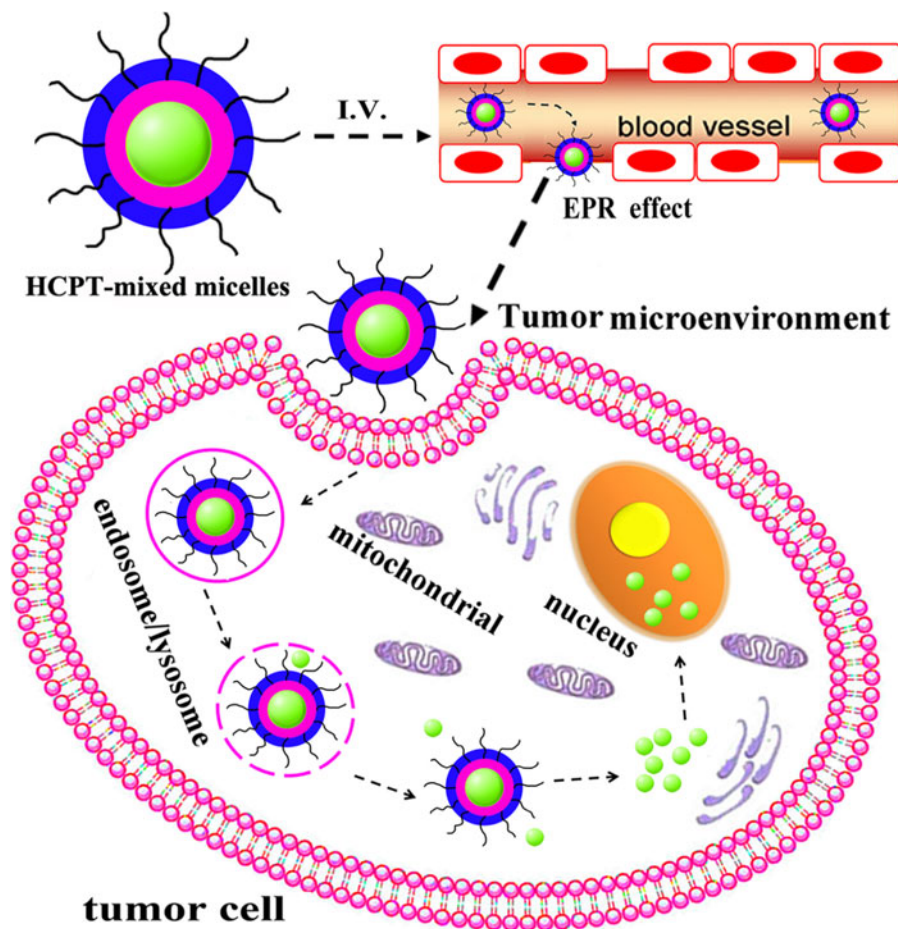
### Materials

10-Hydroxycamptothecin (HCPT) was purchased from Shanghai Beika Medical Technology Co. Ltd. (Shanghai, China). D,L-Lactide and glycolide were purchased from Jinan Daigang Bioengineering Co. Ltd. (Jinan, Shandong, China), and recrystallized by ethyl acetate twice before use. Monomethoxy poly(ethylene glycol) (mPEG, Mn 2000) and stannous octoate were obtained from Sigma-Aldrich Co. (St. Louis, MO, USA). L-Alanine (analytical grade) and pyrene (>99 %) were purchased from Shanghai Biochemical Reagent Company (Shanghai, China) and Fluka Company (St. Louis, MO, USA), respectively. All other reagents were of HPLC or analytical grades.

### Fabrication of blank-mixed micelles

As shown in Scheme 2, mPEG-PLGA was synthesized from ring-opening polymerization using stannous octoate as a catalyst (Beletsi and Leontiadis 1999). Briefly, mPEG (0.6, 0.9, 1.4, or 2.4 mmol), D,L-lactide (0.6 mmol) and glycolide (0.6 mmol) were fused with 0.5 % (w/w) Sn(Oct)<sub>2</sub> in a flask, which had been purged with nitrogen and dried at 180 °C for 12 h. The mixture was maintained at 120 °C under agitation, and the reaction took place for 8 h in nitrogen. To obtain final mPEG-PLGA, the mixture was dissolved in dichloromethane and precipitated in ice-cold diethyl ether; the precipitate was filtered and dried at 45 °C in vacuum. 3(*S*)-methyl-2,5-morpholinedione was synthesized via a two-step reaction (Fung and Glowaky 2003). mPEG-PLGA (0.5 mmol), 3(*S*)-methyl-2,5-morpholinedione (0.5 or 1 mmol) and an aliquot of

**Scheme 1** Illustration of drug accumulation and intracellular trafficking pathway of long-circulating HCPT-mixed micelles. Drug delivery includes steps of intravenous injection, EPR effect, cellular internalization, endosome/lysosome escape, and cytoplasmic release



0.1 mmol/L  $\text{Sn}(\text{Oct})_2$  toluene solution were added to a nitrogen-purged flask pre-heated to 180 °C for 6 h. The reaction took place at 140 °C for 30 min, followed by at 110 °C for 8 h under nitrogen protection. The mixture was then dissolved with tetrahydrofuran and precipitated in petroleum ether. Final polymer PELMD was obtained by filtration and drying.

mPEG-PLGA and PELMD was dissolved in some dimethyl sulfoxide (DMSO), and then dialyzed against distilled water with a molecular weight cut-off (MWCO) of 3500 Da for 24 h at room temperature to form blank-mixed micelles. The outer dialysis phase was replaced with fresh distilled water every 4 h.

Characterization and physicochemical properties of the block copolymers

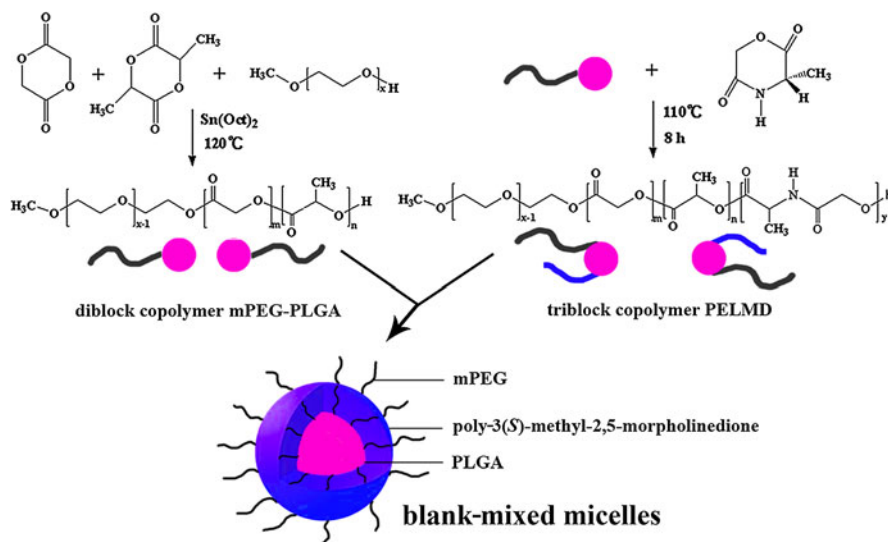
The structures of mPEG-PLGA and PELMD were characterized using  $^1\text{H}$  NMR and FT-IR, respectively.

$^1\text{H}$  NMR was performed on a Bruker Avance AV-500 spectrometer (Karlsruhe, Germany) and FT-IR spectra were recorded on a Bruker Tensor 27 Fourier-transform infrared spectrometer.

Critical micelle concentration (CMC) of PELMD and mPEG-PLGA was determined by a steady-state fluorescence technique using pyrene as an extrinsic probe. In brief, 100- $\mu\text{L}$  pyrene acetone solution was transferred into a volumetric flask and evaporated. Polymers solution ( $5 \times 10^{-9}$  to  $1 \times 10^{-3}$  mg/mL) was then added and equilibrated for 24 h at room temperature in dark. Fluorescence spectra of the polymer were recorded on a Shimadzu RF-5301 PC luminescence spectrometer (Kyoto, Japan). Ratio of fluorescent intensity at 392 and 372 nm ( $I_{392}/I_{372}$ ) was calculated and plotted against logarithm of polymer concentration to obtain the CMC.

Hemolysis of mPEG-PLGA and PELMD was evaluated and compared to low-molecular-weight surfactant Tween 80 as a positive control (Le et al.

**Scheme 2** Polymerization process of the block copolymers and schematic representation of PELMD/mPEG-PLGA-mixed micelles



2004). Two percentage rabbit red blood suspension (v/v, 2.5 mL) was mixed with polymer samples (2.5 mL) of mPEG-PLGA, PELMD or Tween 80 in range of 0.2–4 mg/mL. The supernatant was collected and analyzed for released hemoglobin using a Shimadzu UV-2450 spectrophotometer at 416 nm. Three replicates were utilized for each testing sample.

#### Preparation of long-circulating HCPT-mixed micelles

HCPT-mixed micelles were prepared using a dialysis method, since the polymers were not readily soluble in water. As shown in Fig. 2A, B, PELMD (molar ratio, 3:3:2) or mixture of mPEG-PLGA (molar ratio, 8:2) and PELMD (molar ratio, 3:3:2) was dissolved in 5 mL dimethyl sulfoxide (DMSO); total weight of the copolymers was controlled at 90 mg. HCPT chloroform solution was added drop-wise to the polymer solution. The mixture was stirred at  $35^\circ\text{C}$  for 0.5 h in a water bath, and then dialyzed against distilled water with a molecular weight cut-off (MWCO) of 3,500 Da for 24 h at room temperature. The outer dialysis phase was replaced with fresh distilled water every 4 h. At the conclusion of the dialysis, solution was collected and lyophilized with 3 % mannitol for 24 h to get free-flowing powder of HCPT-mixed micelles for further use.

HCPT-mixed micelles were separated from free HCPT using gel column chromatography. An HPLC system (Shimadzu LC-10AD) coupled with a Diamonsil

$\text{C}_{18}$  column ( $250 \times 4.6$  mm,  $5 \mu\text{m}$ , Dikma Technology Company, China) was used to quantify HCPT in HCPT-mixed micelles. The chromatographic conditions were, mobile phase: methanol:water (60:40, v/v), flow rate: 1.0 mL/min, column temperature:  $30^\circ\text{C}$ , retention time: 8.3 min, detection wavelength: 266 nm, detection limit: 10 ng/mL, calibration range: 1–20  $\mu\text{g}/\text{mL}$ .

Differential scanning calorimetry (DSC) of HCPT-mixed micelles was collected in a DSC-SP Rheometric Scientific differential scanning calorimeter (Piscataway, NJ, USA). Samples were determined in open aluminum pans under a dry nitrogen flow (50 mL/min) and heated at  $-10^\circ\text{C}/\text{min}$  from 30 to  $300^\circ\text{C}$ .

#### Characterization of the mixed micelles

Particle size and zeta potential of the mixed micelles were measured using a Malvern Zetasizer 3000 system (Malvern Instruments Ltd., Malvern, UK). Dynamic light scattering (DLS) measurements were determined at a fixed angle of  $90^\circ$  and at room temperature. Samples were diluted properly before the testing.

Particle morphology of HCPT-mixed micelles was observed using transmission electron microscopy (Hitachi H-7650 electron microscope, Hitachi, Japan). Samples were stained with sodium phosphotungstate solution (2 %, w/w) prior to the experiment.

Stability of HCPT-mixed micelles in aqueous solution was evaluated at  $4^\circ\text{C}$  and  $25^\circ\text{C}$  for 8 days. Particle size and encapsulation efficiency of the mixed

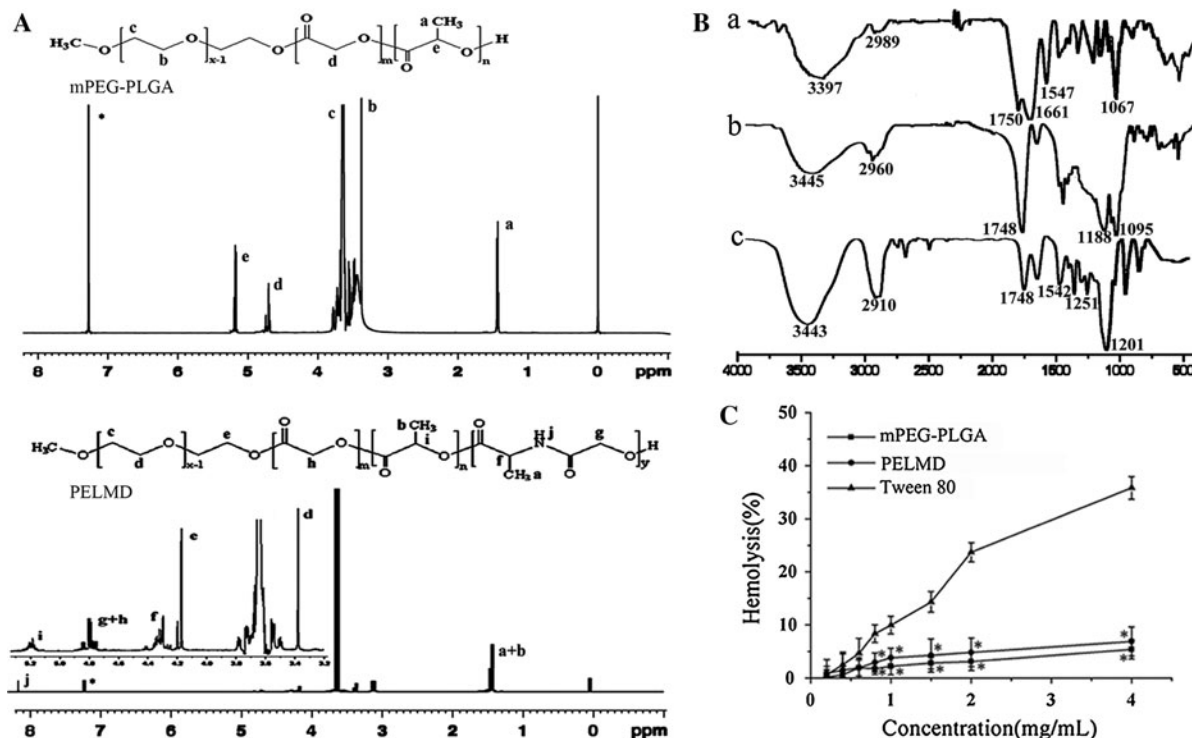


**Fig. 1** A <sup>1</sup>H NMR spectra of mPEG-PLGA and PELMD in CDCl<sub>3</sub>. B FT-IR spectra of 3(S)-methyl-2,5-morpholinedione (a), mPEG-PLGA (b), and PELMD (c). C Hemolysis of mPEG-

PLGA, PELMD, and positive control Tween 80 at different use concentrations (mean ± SD, n = 3, \*significant difference from Tween 80, P < 0.05)

micelles were measured on 0, 2, 4, 6, and 8 days by particle sizer and HPLC respectively.

Release of HCPT from the mixed micelles and PELMD micelles was measured using a dialysis method. One millilitre of pre-filtered micelles was transferred into a dialysis pocket (MWCO 8,000–10,000, Spectra/Por, Houston, TX, USA) and placed in 100 mL PBS solution (pH 5.0, 6.5, or 7.4) containing 0.02 % (w/v) Tween 80 (Zhang et al. 2007). The release test was conducted at 37 °C and 100 rpm for 96 h, and each test was run in triplicates. At predetermined intervals, 2 mL samples were collected and HCPT concentration was quantified using the HPLC method previously described.

Pharmacokinetics and biodistribution of HCPT-mixed micelles

Healthy Sprague–Dawley (SD) rats (250 ± 20 g) and Kunming mice (25 ± 5 g) were obtained from Center for New Drug Screening, China Pharmaceutical University. The animal use protocol was approved

by the Ethics Board of China Pharmaceutical University, and all experiments were carried out in accordance to guidelines set by the Chinese Council on Animal Care. Study animals were housed in pathogen-free facility and provided food and water ad libitum.

Pharmacokinetics of HCPT-mixed micelles was evaluated in SD rats. Twelve rats were randomly divided into two groups; one group received HCPT-mixed micelles injection and the other received HCPT control injection. Drug dosing was 5 mg HCPT/kg body weight, intravenous administration through the tail vein. Blood samples were collected from orbital plexus at 5, 10, 15, 20, 30 min, and 1, 2, 3, 4, 6, 8, 12 h after dosing. The samples were centrifuged immediately at 3,000 rpm for 10 min; plasma samples were separated and frozen at –20 °C until drug analysis. Study animals were euthanized with ether at the conclusion of the experiment.

Biodistribution of HCPT-mixed micelles was evaluated in Kunming mice, using the same drug dosing regimen and HCPT control injection. The study animals were sacrificed at 0.25, 0.5, 1, 2, 4 h after dosing, tissue samples including heart, liver, spleen,

lung, and kidney were harvested. The specimens were weighed, washed with saline, and homogenized before frozen at  $-20\text{ }^{\circ}\text{C}$  for further drug analysis.

To determine HCPT level in biological samples, 200- $\mu\text{L}$  sample was mixed with 40- $\mu\text{L}$  internal standard 7-ethyl-10-hydroxycamptothecin (SN-38, 40  $\mu\text{g}/\text{mL}$ ). The mixture was acidified with 20- $\mu\text{L}$  glacial acetic acid, and kept in dark for 2 h. Three millilitre ethyl acetate was added to the sample, vortexed for 2 min and centrifuged at 8,000 rpm for 10 min to extract HCPT. Supernatant was collected and dried under nitrogen stream, reconstituted with 100  $\mu\text{L}$  methanol, centrifuged at 8,000 rpm for another 10 min before HPLC analysis.

An HPLC system (Shimadzu LC-10AD) coupled with a Diamonsil  $\text{C}_{18}$  column (250  $\times$  4.6 mm, 5  $\mu\text{m}$ ) was used to quantify HCPT in biological samples. The chromatographic conditions were, mobile phase: methanol:water (55:45, v/v, pH 5.0), flow rate: 1.0 mL/min, column temperature: 30  $^{\circ}\text{C}$ , retention time: 9.8 min, detection wavelength: 384 nm, detection limit: 8 ng/mL, calibration range: 0.05–10  $\mu\text{g}/\text{mL}$  (plasma).

#### Data analysis

Experimental results were expressed as mean  $\pm$  standard deviation (SD) unless otherwise noted. Pharmacokinetic and biodistribution parameters were calculated using DAS 2.0 Pharmacokinetics Software (Chinese Society of Mathematical Pharmacology) with compartmental or non-compartmental methods. One-way analysis of variance (ANOVA, SPSS Version 11.5) was used to compare all data; statistical significance was considered at  $P < 0.05$ .

## Results and discussion

Numerous factors may influence efficient specific drug targeting and delivery to tumor sites; one of the most critical factors is to make the preparation adaptable to physiological tumor environment and subsequently survive extracellular elimination in vivo (Danquah et al. 2011). For example, nanocarriers conjugated with ligands were capable of active drug targeting by interacting with receptors overexpressed on tumor cells (Yadav et al. 2007; Shen et al. 2012). Nanocarriers of pH-sensitive components could also increase

passive tumor targeting by manipulating mildly acidic tumor microenvironment in pH 6.0–7.0 (Kim et al. Kim et al. 2010; Zhao et al. 2011). Micelles prepared from single copolymers were often lacking flexibility due to limitations in selecting building blocks. On the other hand, mixed micelles assembled from two or more block copolymers provided efficient and convenient approaches to enhance thermodynamic and kinetic stability (Kim et al. 2009). Researchers have found advantages in improving drug-loading (Wang et al. 2007; Yang et al. 2009), incorporating multiple functionalities (Yoo and Park 2004), and preventing particle precipitation (Alakhov et al. 1999) without the need for utilizing complex synthetic schemes. In this study, we selected two biocompatible and biodegradable copolymers PELMD and mPEG–PLGA to prove this research rationale.

#### Fabrication of blank-mixed micelles

Scheme 2 shows the preparation pathways of the blank-mixed micelles. mPEG–PLGA were melt-polymerized by D,L-lactide, glycolide, and mPEG, while PELMD was further formed by ring-opening copolymerization of 3(*S*)-methyl-2,5-morpholinedione and mPEG–PLGA. 3(*S*)-Methyl-2,5-morpholinedione was one of the 2,5-morpholinedione derivatives that may alter copolymers of  $\alpha$ -amino acids and  $\alpha$ -hydroxy acids (Tian et al. 2003); these compounds were known to be nontoxic and biodegradable, and were often utilized to introduce polypeptide structure into polymers. mPEG–PLGA and PELMD self-assembled into mixed micelles to enhance the advantages of nano-delivery system.

#### Characteristics and physicochemical properties of the block polymers

Copolymerization of mPEG–PLGA and PELMD was confirmed by  $^1\text{H}$  NMR assay. Figure 1A shows the  $^1\text{H}$  NMR spectra of both copolymers. Peaks of mPEG–PLGA were consistent to those previously reported (Wang et al. 2011), and they were assigned as follows: 1.57 (O–CH–CH<sub>3</sub>, 3H, PLGA segment), 3.3–3.8 (O–CH<sub>2</sub>–CH<sub>2</sub>, 4H PEG segment), 4.8 (O–CH<sub>2</sub>–CO, 2H, PLGA segment), 5.2 (O–CH–CH<sub>3</sub>, 1H, PLGA segment). Comparing spectrum of PELMD to that of mPEG–PLGA, chemical shifts of triblock copolymer

showed up-field shift of N–H signal from 7.15 to 6.9 ppm.

Figure 1B shows FT-IR spectrum of 3(*S*)-methyl-2,5-morpholinedione, mPEG–PLGA and PELMD; the three spectra demonstrated similar characteristic peaks as the substances basically possessed same functional groups. PELMD presented a broad –OH and N–H stretch absorption band between 3,200 and 3,445  $\text{cm}^{-1}$ . A strong band at 1,748  $\text{cm}^{-1}$  belonged to carbonyl group in both PLGA and poly-3(*S*)-methyl-2,5-morpholinedione segments. Signals at 1,644 and 1,542  $\text{cm}^{-1}$  indicated amide group in 3(*S*)-methyl-2,5-morpholinedione unit. Absorption at 1,251 and 1,102  $\text{cm}^{-1}$  were assigned to ester group in PLGA chain, and the newly appeared peak at 1,201  $\text{cm}^{-1}$  was an indicator of ester group in poly-3(*S*)-methyl-2,5-morpholinedione segment. Based on spectra of  $^1\text{H}$  NMR and FT-IR, it was concluded that mPEG–PLGA and PELMD had been successfully synthesized.

CMC plays an important role in maintaining stability of various drug delivery systems. Table 1 lists CMCs of mPEG–PLGA and PELMD at variable structural compositions. By introducing poly-3(*S*)-methyl-2,5-morpholinedione to mPEG–PLGA, CMC values of the triblock copolymer PELMD were lowered by three to five times. CMC values of all copolymers tested were approximately 200 times lower than that of low molar mass surfactant, e.g., 1 g/L of poloxamer (Prasad et al. 1979). Similar to previous findings (Yamamoto et al. 2002), the higher the poly-3(*S*)-methyl-2,5-morpholinedione segment ratio was, the lower the CMC values could be determined. Interactions of polydesipeptide among polymer molecules could reduce core fluidity and subsequently enhance nanoparticle stability. Results hence suggested that PELMD and mPEG–PLGA could form stable nanoparticles in aqueous medium and retain sufficient stability even after dilution by blood circulation after intravenous administration.

Behaving as surfactants, amphiphilic polymers will induce damages to cell membrane after intravenous administration (Le et al. 2004). Hemolytic effects of mPEG–PLGA and PELMD on rabbit red blood cells were tested and compared to Tween 80, and Fig. 1C shows the results. Hemolysis induced by mPEG–PLGA and PELMD was significantly different from Tween 80 at concentrations ranging 0.8–4 mg/mL; at 4 mg/mL Tween 80 was 36 % hemolytic whereas both copolymers were non-hemolytic in vitro. Results from

this experiment suggested that mPEG–PLGA and PELMD demonstrated satisfactory safety in hemolysis that could be further prepared as injectable nanoparticles.

#### Self-assemble of HCPT-mixed micelles

HCPT is poorly soluble in water and other physiologically compatible pharmaceutical solvents. Self-assembled micelles would dramatically enhance HCPT aqueous solubility, thus prolonging its circulation time in blood once injected. HCPT-mixed micelles were prepared using a dialysis method in this study (Fig. 2A, B). Table 2 lists various characteristics of HCPT-mixed micelles with different copolymer compositions; optimal charge ratio between mPEG–PLGA and PELMD was found to be 1:1. When charge ratio was increased, particle size, entrapment efficacy, and drug loading of the resultant HCPT-mixed micelles would all decrease. The tested HCPT-mixed micelles were suitable for lyophilization with 3 % mannitol, indicating its feasibility for an injectable formulation.

To confirm the entrapment of HCPT within the polymeric micelles, DSC analysis was carried out for free HCPT, blank micelles, HCPT-mixed micelles, and physical mixture of blank micelles and HCPT (Fig. 2C). Broadening melting peak was observed at around 102.5 °C for free HCPT (a) and 97.3 °C for physical mixture of blank micelles and free HCPT (c), respectively. The characteristic signal disappeared in blank micelles (b) and HCPT-mixed micelles (d), implying homogeneous entrapment of HCPT within the micelles once prepared.

#### Characterization of HCPT-mixed micelles

Surface charge is a critical attribute to physical stability in a dispersed system. High surface charges

**Table 1** Critical micelle concentrations (CMC) of block copolymers mPEG–PLGA and PELMD at variable composition in deionized water

mPEG–PLGA	CMC (mg/L)	PELMD	CMC (mg/L)
8:2 <sup>a</sup>	4.91	3:3:1 <sup>a</sup>	0.71
7:3	4.78	3:3:2	0.48
6:4	3.42	3:2:1	1.01

<sup>a</sup> Feed ratio of the polymers

may create repelling forces among the dispersing particles, increasing overall stability of the solution (Kwon et al. 2003). Zeta potentials of mPEG–PLGA

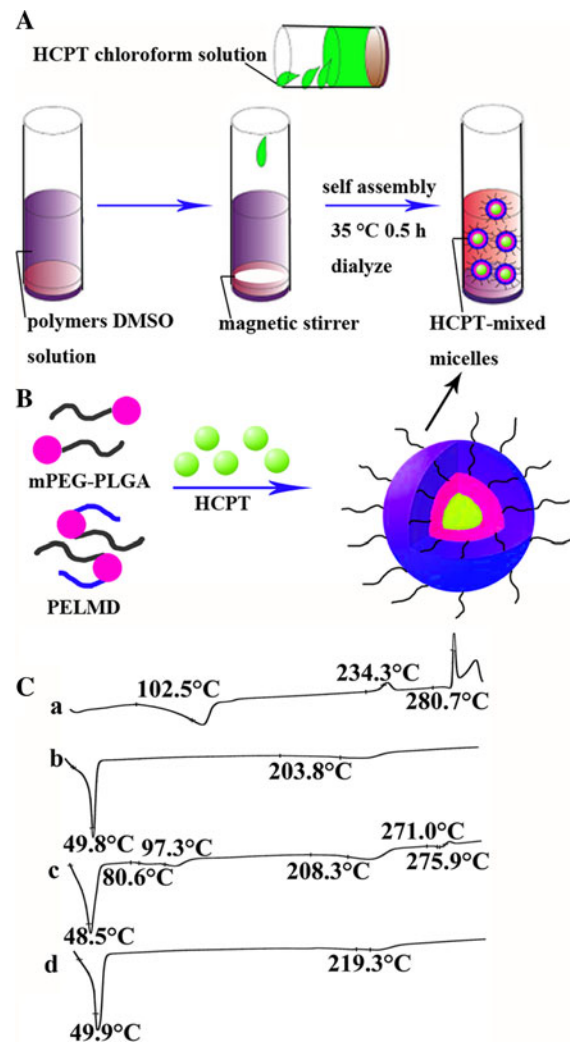


**Fig. 2** **A** Fabrication of HCPT-mixed micelles. **B** Schematic representation of HCPT-loaded PELMD/mPEG–PLGA-mixed micelles. **C** DSC thermograms of free HCPT (*a*), empty micelles (*b*), physical mixture of HCPT (5 %)/empty micelles (*c*), and HCPT-mixed micelles (*d*)

nanoparticles tended to range in lower negativity (Gryparis et al. 2007). In this study zeta potentials of the mixed micelles were measured in positive values, which was attributed to the introduction of polydesipeptide in the polymers. At an optimal charge ratio of 1:1, average particle size of HCPT-mixed micelles was approximately 160 nm with a desirable polydispersity index of 0.135 (Fig. 3A); drug entrapment efficiency was also significantly higher than that of the other two micelles studied. It appeared that the charged particles could adequately repel each other and prevent aggregation or precipitation from happening, thus leading to satisfactory preparation stability (Hunter 1981).

The prepared HCPT-mixed micelles were directly visualized for their particle size and morphology using TEM, and Fig. 3B shows two typical sample photos. The drug-loaded mixed micelles were spherical with a core–shell structure, and the size distribution was relatively uniform. Because of dehydration and subsequent shrinkage of the particles used for preparing TEM samples (Zhou et al. 2010), measurement obtained from this experiment was smaller than the hydrodynamic diameter obtained from DLS experiment. The dark halo around the mixed micelles may be caused by selective affinity of the water-soluble staining agent for PEG shells. The uniform particle size distribution and core–shell structure enhanced the physical stability of the drug delivery system and minimized the potential for the drug to migrate outside of the micelles.

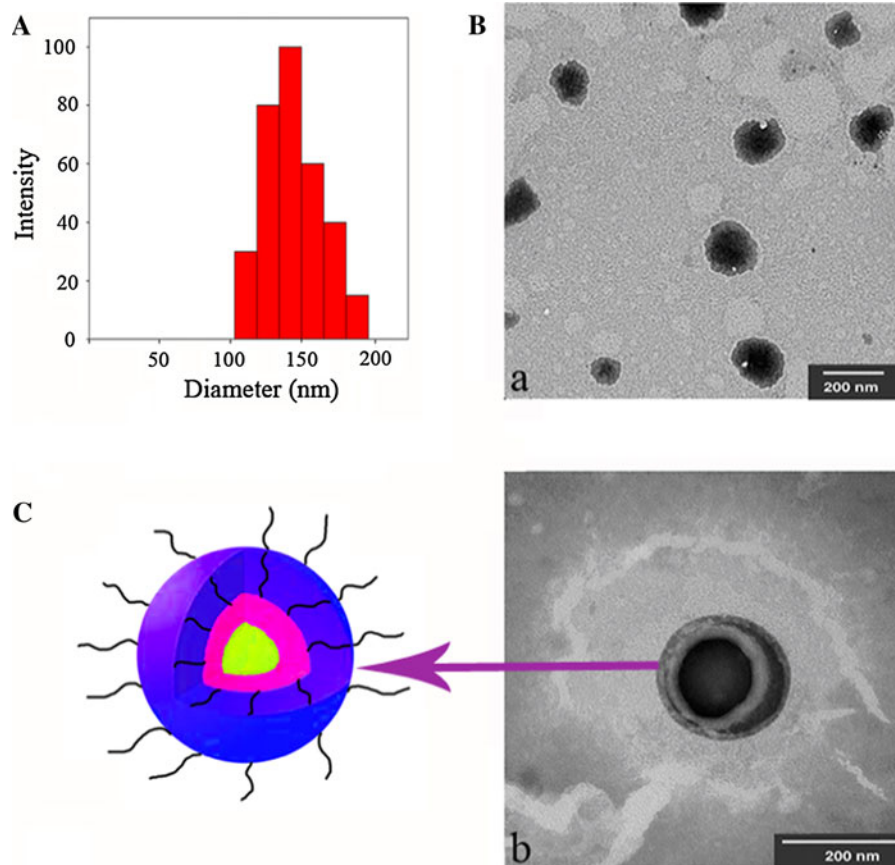
Figure 4A shows the effects of storage time and temperature on stability of HCPT-mixed micelles solution. No significant change was observed in particle size and drug entrapment efficiency when the samples were stored at 4 °C for 8 days. At room temperature, however, drug entrapment efficiency of the mixed micelles decreased from 88 to 53 % within the test interval while average particle diameter doubled, indicating stability issues for the preparation

**Table 2** Characteristics of HCPT-mixed micelles prepared from mPEG–PLGA and PELMD (mean  $\pm$  SD,  $n = 3$ )

HCPT-mixed micelles	Particle size (nm)	Polydispersity index ( $\mu_2/\Gamma^2$ )	Zeta potential (mV)	Entrapment efficiency (%)	Drug loading (%)
1:1 <sup>a</sup>	165.1 $\pm$ 3.6	0.135	+15.3 $\pm$ 0.5	86.8 $\pm$ 1.7	8.8 $\pm$ 0.1
1:2	198.8 $\pm$ 2.8	0.199	+17.4 $\pm$ 1.9	71.9 $\pm$ 3.7	7.4 $\pm$ 0.2
1:4	203.9 $\pm$ 4.3	0.217	+19.6 $\pm$ 2.2	60.5 $\pm$ 2.3	6.3 $\pm$ 0.1

<sup>a</sup> Feed ratio of mPEG–PLGA and PELMD

**Fig. 3** **A** Size distribution and **B** transmission electron microscopy (TEM) measurement of HCPT-mixed micelles (*a, b*), and the corresponding schematic representation of HCPT-mixed micelles (*c*)



at elevated temperature. By introducing polydesipeptide, surface charge of the resultant HCPT-mixed micelles was positive and relatively high, which would provide a strong repelling force between the particles for improved physical stability. In addition, hydrophobic and electrostatic interactions between the two copolymers may also enhance kinetic stability and redispersion properties of HCPT-mixed micelles (Atia et al. 2011).

As a novel drug delivery system, nanocarriers are capable of improving specific drug targeting and minimizing drug side effect and/or toxicity to normal tissues by EPR effects (Torchilin 2006; Zhao et al. 2010). Modified drug release from mixed micelles is critical in efficient delivering anticancer compounds to tumor sites. Figure 4B shows HCPT release from HCPT-mixed micelles under different pH conditions. Drug release at lower pH conditions (5.0 and 6.5) was faster than that at pH 7.4; the cumulative drug release amount from the mixed micelles at 10 h was 1.7 times at pH 5.0 and 1.4 times at pH 6.5 of that at pH 7.4. By

the conclusion of dissolution experiment at 96 h, cumulative drug release of the mixed micelles at pH 5.0, 6.5, and 7.4 was 76.8, 72.1, and 61.3 %, respectively. HCPT release from PELMD micelles also demonstrated a pH-dependent profile, but drug release was further suppressed in comparison to that of the mixed micelles, i.e., 53.7 % HCPT was still entrapped at pH 5.0 after 96 h. The pH-dependent release of HCPT-mixed micelles would be especially desirable for antitumor compounds, since pH conditions at tumor sites tend to be lower than those of the normal tissues. This would allow reduced drug release at normal physiological pH conditions, leading to more drug transport and delivery at tumor sites (Mo et al. 2012). Modified drug release at different pH conditions was likely attributed to introduction of polydesipeptide to the polymers. The selective drug release characteristics would also be beneficial in reducing toxicity to normal tissues and improving therapeutic outcomes with more concentrated drug concentration at specific tissue target.

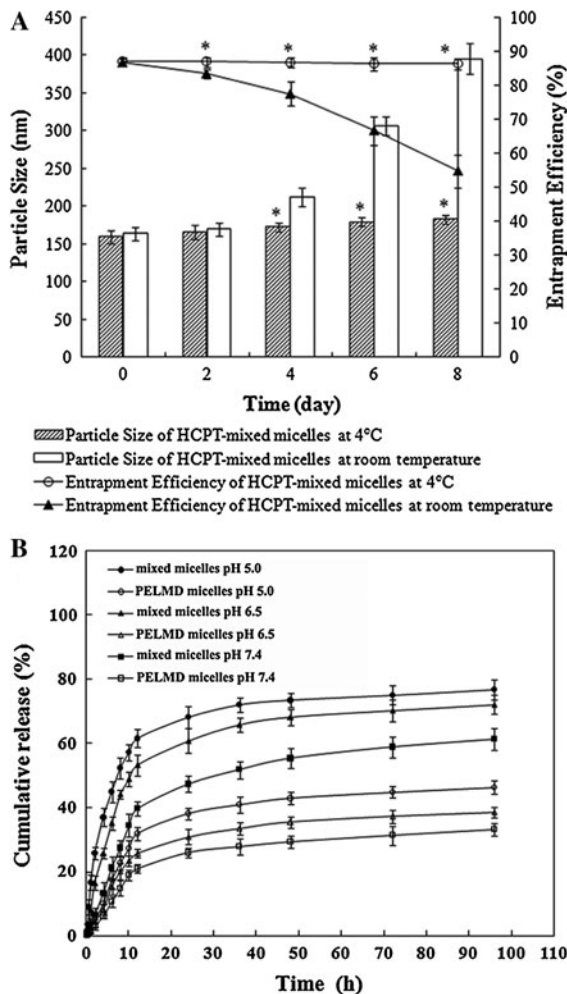


**Fig. 4** **A** Changes of particle size and entrapment efficiency of HCPT-mixed micelles at 4 or 25 °C (mean  $\pm$  SD,  $n = 3$ , \* significant difference from HCPT-mixed micelles stored at 25 °C,  $P < 0.05$ ). **B** HCPT release profiles from HCPT-mixed micelles under different pH conditions (mean  $\pm$  SD,  $n = 3$ )

#### Pharmacokinetics and biodistribution of HCPT-mixed micelles

A comparative pharmacokinetic study was carried out in rats and plasma drug concentrations after a single intravenous administration of HCPT injection or HCPT-mixed micelles were measured using HPLC. Figure 5 shows the plasma concentration–time curves of the study, and Table 3 lists primary pharmacokinetic parameters obtained by compartment and non-compartment analysis. One of the critical criteria for efficient drug targeting is to prolong drug circulation time so that drug payload could reach tumor site at a

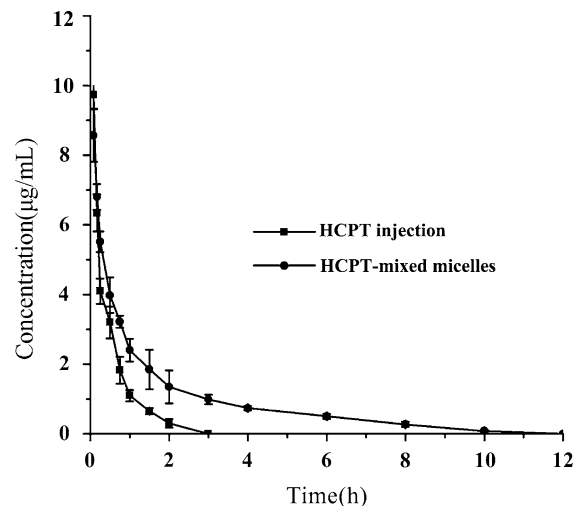


**Fig. 5** HCPT plasma concentration–time profiles following intravenous administration of HCPT injection and HCPT-mixed micelles at 5 mg/kg in rats (mean  $\pm$  SD,  $n = 6$ )

**Table 3** Pharmacokinetic parameters of HCPT following intravenous administration of HCPT injection and HCPT-mixed micelles at 5 mg/kg in rats (mean  $\pm$  SD,  $n = 6$ )

Parameters	HCPT injection	HCPT-mixed micelles
$t_{1/2}^a$ (h)	0.31 $\pm$ 0.05	1.98 $\pm$ 0.23*
$AUC_{0 \rightarrow t}^b$ ( $\mu\text{g}/\text{mLh}$ )	3.52 $\pm$ 0.39	12.25 $\pm$ 1.52*
$AUC_{0 \rightarrow \infty}^c$ ( $\mu\text{g}/\text{mLh}$ )	3.64 $\pm$ 0.48	12.56 $\pm$ 1.55*
$CL^d$ (L/h)	0.26 $\pm$ 0.03	0.09 $\pm$ 0.02*
$MRT_{0 \rightarrow \infty}^e$ (h)	0.39 $\pm$ 0.06	2.55 $\pm$ 0.02*

\* Significant difference from HCPT injection,  $P < 0.05$

<sup>a</sup> The elimination half-life

<sup>b</sup> The area under the plasma drug concentration versus time curve from 0 to  $t$  ( $t = 12$  h)

<sup>c</sup> The total area under the plasma drug concentration versus time curve from 0 to infinity

<sup>d</sup> The plasma clearance

<sup>e</sup> The mean residence time of drug in plasma

significantly therapeutic amount. While HCPT concentration from regular HCPT injection was below the quantification limit 2 h after the administration, HCPT concentration from the mixed micelles was still detectable 10 h after the administration. All pharmacokinetic parameters from HCPT-mixed micelles were significantly different from those of the conventional injection. In particular, plasma elimination half-life and area under the concentration–time curve ( $AUC_{0 \rightarrow \infty}$ ) were increased by 6.4 and 3.6 folds in

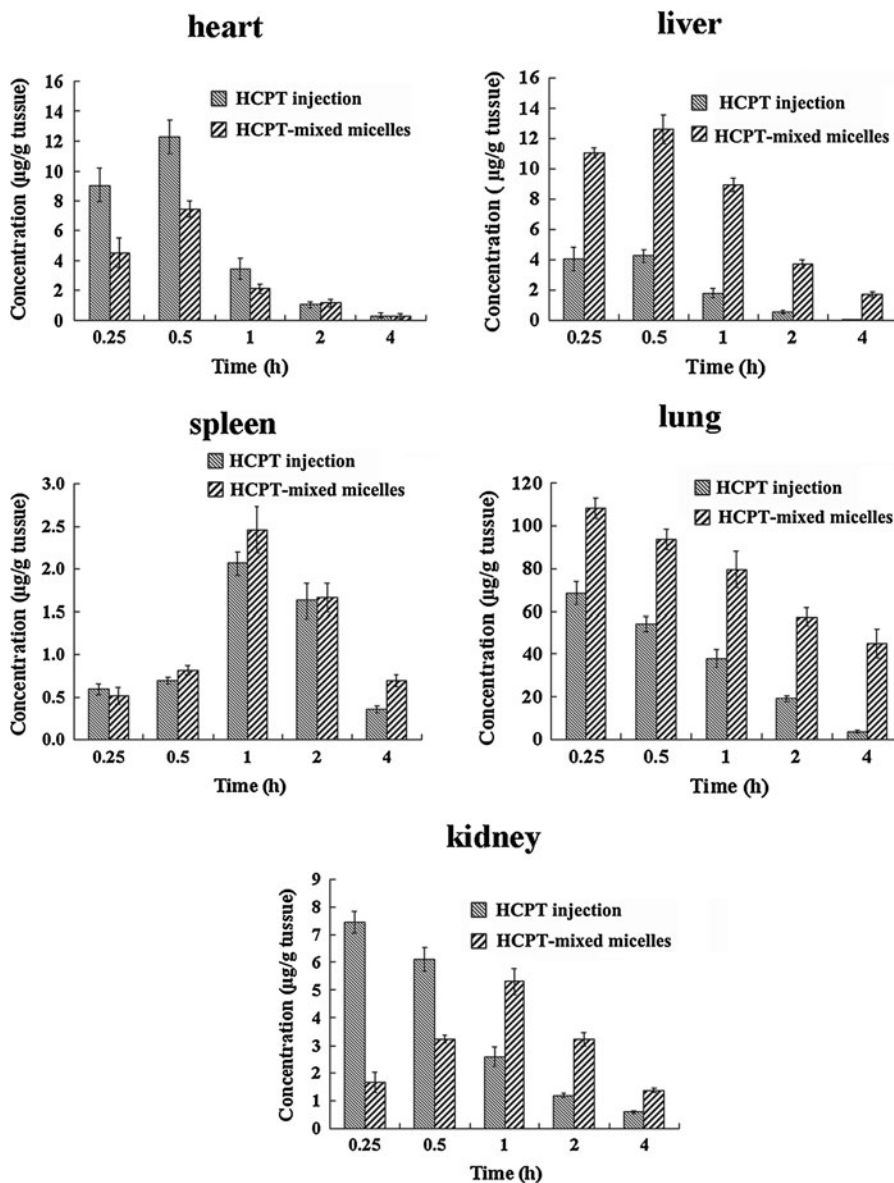


**Fig. 6** Tissue biodistribution of HCPT following intravenous administration of HCPT injection and HCPT-mixed micelles at 5 mg/kg in mice (mean ± SD, n = 6)

comparison to HCPT injection. Mean residence time ( $MRT_{0 \rightarrow \infty}$ ) of HCPT in mixed micelles was prolonged for 6.5 times in comparison to HCPT injection. The clearance of HCPT-mixed micelles was approximately 0.4-fold of that of HCPT injection. The results confirmed the hypothesis that nanocarriers with a steric PEG barrier could prevent rapid drug uptake and elimination, prolong circulation half-life, and increase EPR effect, which would further potentiate passive

drug targeting to non-MPS disease regions such as tumor tissues (Vonarbourg et al. 2006; Parveen and Sahoo 2011). High density PEGs have been utilized to coat nanoparticle surface so that the resultant preparation would effectively remain in blood longer. Mixed micelles tested in this study were composed of two polymers, and both were mixed at variable proportions to produce desirable properties for anti-cancer drug HCPT. The hydrophobic and electrostatic

**Table 4** AUC and MRT of HCPT in tissues following intravenous administration of HCPT injection and HCPT-mixed micelles at 5 mg/kg in mice (mean  $\pm$  SD,  $n = 6$ )

Tissues	HCPT injection		HCPT-mixed micelles	
	AUC <sub>0→∞</sub> <sup>a</sup> (μg/gh)	MRT <sub>0→∞</sub> <sup>b</sup> (h)	AUC <sub>0→∞</sub> (μg/gh)	MRT <sub>0→∞</sub> (h)
Heart	12.42 $\pm$ 0.71	0.94 $\pm$ 0.16	8.02 $\pm$ 0.69*	1.22 $\pm$ 0.31*
Liver	5.35 $\pm$ 0.53	0.81 $\pm$ 0.05	22.84 $\pm$ 1.03*	1.74 $\pm$ 0.08*
Spleen	4.82 $\pm$ 0.35	2.09 $\pm$ 0.10	5.53 $\pm$ 0.37*	2.84 $\pm$ 0.28*
Lung	109.65 $\pm$ 5.11	1.25 $\pm$ 0.08	269.21 $\pm$ 5.52*	5.44 $\pm$ 2.09*
Kidney	9.62 $\pm$ 0.43	1.59 $\pm$ 0.18	8.44 $\pm$ 0.54*	2.84 $\pm$ 0.42*

\* Significant difference from HCPT injection,  $P < 0.05$

<sup>a</sup> The total area under the tissue drug concentration versus time curve from 0 to infinity

<sup>b</sup> The mean residence time of drug in the tissue from 0 to infinity

interactions between mPEG–PLGA and PELMD in HCPT-mixed micelles were essential in enhancing in vivo kinetic stability and pharmacokinetics.

Biodistribution of HCPT-mixed micelles in major tissues after intravenous administration was also examined in a mouse model. Figure 6 shows HCPT biodistribution in major organs including heart, liver, spleen, lung, and kidney. HCPT-mixed micelles were found primarily in liver and lung after drug administration, maximum HCPT concentration in the two organs was 2.9 and 1.6 folds of the HCPT injection, respectively. On the other hand, HCPT injection produced more drug distribution to heart and kidney, its maximum HCPT concentration in these two organs was 1.6 and 2.2 folds of the mixed micelles, respectively. Favorable distribution of HCPT-mixed micelles in lung might be attributed to appropriate particle size and unique properties of mixed micelles assembled from copolymers mPEG–PLGA and PELMD. Table 4 also lists AUC<sub>0→∞</sub> and MRT<sub>0→∞</sub> of HCPT in these organs. There were significant differences between the two test preparations in terms of drug concentration and retention time. The MRT<sub>0→∞</sub> value of the mixed micelles was all extended in comparison to that of HCPT injection. Compared with HCPT injection, MRT<sub>0→∞</sub> values of HCPT from mixed micelles in liver and lung were longer (2.2 and 4.4 folds); and in heart, spleen, and kidney, MRT values for mixed micelles were 1.3, 1.4, and 1.8 folds of the counterparts from the injection. This change was likely induced by stronger electrostatic interactions between positively charged HCPT-mixed micelles and negatively charged tissue cells, subsequently leading to slower elimination rate from

the tissues. Similarly, AUC<sub>0→∞</sub> values from mixed micelles in liver and lung were 4.3 and 2.5 folds of those from HCPT injection. Interestingly, AUC values from HCPT-mixed micelles in heart and kidney were only 0.7 and 0.9 times of the counterparts from HCPT injection, potentially reducing HCPT toxicity to the tissues. It was reasonable to deduce that the mixed micelles would improve intracellular drug release to increase antitumor efficiency, after having targeted tumor tissues and cells by EPR effect. In addition, HCPT-mixed micelles could easily avoid mononuclear phagocyte system (MPS) trapping and sustain a long circulation time in vivo, which would further increase their passive targeting potential to non-MPS disease regions. The animal study results suggested that the mixed micelles might possess important clinical attributes in anticancer drug delivery through reduced toxicity in heart and kidney and accumulated concentration in liver and lung. Further animal studies are ongoing to assess efficacy and safety of HCPT-mixed micelles in various cancer models.

## Conclusions

A novel nanocarrier drug delivery system based on copolymers PELMD and mPEG–PLGA was prepared and tested in this study. The amphiphatic copolymers self-assembled to form mixed micelles through hydrophobic and electrostatic interactions. Using anticancer compound HCPT as a model drug, the drug-loaded mixed micelles were evaluated both in vitro and in vivo. Drug release from HCPT-mixed micelles was pH-dependent, with accelerated release at lower pH

environment. Systemic retention of HCPT-mixed micelles was also prolonged in comparison to conventional injection in animal models, with specific drug accumulation in liver and lung. The mixed micelles also demonstrated enhanced preparation stability and satisfactory safety. Results from this study suggested that this nanodrug delivery system could be applicable for other physicochemically unstable and/or highly toxic antitumor compounds. Further studies are ongoing to elucidate its cellular uptake mechanisms and pharmacodynamics in cancer-bearing animal models.

**Acknowledgments** The authors acknowledge financial support from the Key New Drug Innovation Program, the Ministry of Science and Technology (No. 2009ZX 09310-004 and No. 2009ZX09502-004).

## References

- Alakhov V, Klinski E, Li SM, Pietrzynski G, Venne A, Batrakova E, Bronitch T, Kabanov A (1999) Block copolymer-based formulation of doxorubicin. From cell screen to clinical trials. *Colloid Surf B* 16:34–113. doi:10.1016/S0927-7765(99)00064-8
- Alexis F, Pridgen E, Molnar LK, Farokhzad OC (2008) Factors affecting the clearance and biodistribution of polymeric nanoparticles. *Mol Pharm* 5:505–515. doi:10.1021/mp800051m
- Attia ABE, Ong ZY, Hedrick JL, Lee PP, Ee PLR, Hammond PT, Yang YY (2011) Mixed micelles self-assembled from block copolymers for drug delivery. *Cur Opin Col Inter Sci* 16:182–194. doi:10.1016/j.cocis.2010.10.003
- Beletsi A, Leontiadis L (1999) Effect of preparative variables on the properties of poly (D,L-lactide-co-glycolide)-methoxy-poly-(ethyleneglycol) copolymers related to their application in controlled drug delivery. *Int J Pharm* 182:187–197. doi:10.1016/S0378-5173(99)00058-7
- Chen N, Debnath J (2010) Autophagy and tumorigenesis. *FEBS Lett* 584:1427–1435. doi:10.1016/j.febslet.2009.12.034
- Chen W, Chen H, Hu J, Yang W, Wang C (2006) Synthesis and characterization of poly ion complex micelles between poly(ethylene glycol)-grafted poly(aspartic acid) and cetyltrimethyl ammonium bromide. *Colloids Surf A* 278:60–66. doi:10.1016/j.colsurfa.2005.11.084
- Chen J, He H, Li S, Shen Q (2011) An HPLC method for the pharmacokinetic study of vincristine sulfate-loaded PLGA-PEG nanoparticle formulations after injection to rats. *J Chromatogr B* 879:1967–1972. doi:10.1016/j.jchromb.2011.05.031
- Danquah MK, Zhang XA, Mahato RI (2011) Extravasation of polymeric nanomedicines across tumor vasculature. *Adv Drug Deliver Rev* 63:623–639. doi:10.1016/j.addr.2010.11.005
- Esmaili F, Ghahremani MH, Esmaili B, Khoshayand MR, Atyabi F, Dinarvand R (2008) PLGA nanoparticles of different surface properties: preparation and evaluation of their body distribution. *Int J Pharm* 349:249–255. doi:10.1016/j.ijpharm.2007.07.038
- Fernández-Carballido A, Pastoriza P, Barcia E, Montejo C, Negro S (2008) PLGA/PEG-derivative polymeric matrix for drug delivery system applications: characterization and cell viability studies. *Int J Pharm* 352:50–57. doi:10.1016/j.ijpharm.2007.10.007
- Fung FN, Glowaky RC (2003) Bioabsorbable polydepsipeptides, their preparation and use. EP0322154A2
- Gryparis EC, Hatzia Apostolou M, Papadimitriou E, Avgoustakis K (2007) Anticancer activity of cisplatin-loaded PLGA-mPEG nanoparticles on LNCaP prostate cancer cells. *Eur J Pharm Biopharm* 67:1–8. doi:10.1016/j.ejpb.2006.12.017
- Han G, Ghosh P, Rotello V (2007) Functionalized gold nanoparticles for drug delivery. *Nanomedicine* 2:113–123. doi:10.1166/jbn.2013.1536
- Hunter RJ (1981) Zeta potential in colloid science: principles and applications. Academic Press, New York
- Kim S, Tan J, Nederberg F, Fukushima K, Yang Y, Waymouth RM, Hedrick JL (2009) Mixed micelle formation through stereocomplexation between enantiomeric poly (lactide) block copolymers. *Macromolecules* 42:25–29. doi:10.1021/ma801739x
- Kim J, Garripelli VK, Jeong U, Park J, Repka MA, Jo S (2010) Novel pH-sensitive polyacetal-based block copolymers for controlled drug delivery. *Int J Pharm* 401:79–86. doi:10.1016/j.ijpharm.2010.08.029
- Kwon S, Park JH, Chung H, Kwon IC, Jeong SY (2003) Physicochemical characteristics of self-assembled nanoparticles based on glycol chitosan bearing 5β-cholanic acid. *Langmuir* 19:10188–10193. doi:10.1021/la0350608
- Le GD, Gori S, Luo L, Lessard D, Smith DC, Yessine MA, Ranger M, Leroux JC (2004) Poly(N-vinylpyrrolidone)-block-poly(D,L-lactide) as a new polymeric solubilizer for hydrophobic anticancer drugs: in vitro and in vivo evaluation. *J Control Release* 99:83–101. doi:10.1016/j.jconrel.2004.06.018
- Lo C, Chang Y, Wu S, Lee C (2010) Effect of particle size on the phase behavior of block copolymer/nanoparticle composites. *Colloid Surface A* 368:6–12. doi:10.1016/j.colsurfa.2010.06.027
- Maeda H, Wu J, Sawa T, Matsumura Y, Hori K (2000) Tumor vascular permeability and the EPR effect in macromolecular therapeutics: a review. *J Control Release* 65:271–284. doi:10.1016/S0168-3659(99)00248-5
- Mo R, Sun Q, Xue J, Li N, Li W, Zhang C, Ping Q (2012) Multistage pH-responsive liposomes for mitochondrial-targeted anticancer drug delivery. *Adv Mater* 24:3659–3665. doi:10.1002/adma.201201498
- Moghimi SM, Hunter AC, Murray JC (2001) Long-circulating and target-specific nanoparticles: theory to practice. *Pharmacol Rev* 53:283–318. doi:0031-6997/01/5302-283-318
- Niu J, Su Z, Xiao Y, Huang A, Li H, Bao X, Li S, Chen Y, Sun M, Ping Q (2012) Octreotide-modified and pH-triggering polymeric micelles loaded with doxorubicin for tumor targeting delivery. *Eur J Pharm Sci* 45:216–226. doi:10.1016/j.ejps.2011.11.013
- Pan X, Yao P, Jiang M (2007) Simultaneous nanoparticle formation and encapsulation driven by hydrophobic

- interaction of casein-graft-dextran and  $\beta$ -carotene. *J Colloid Interf Sci* 315:456–463. doi:[10.1016/j.jcis.2007.07.015](https://doi.org/10.1016/j.jcis.2007.07.015)
- Parveen S, Sahoo SK (2011) Long circulating chitosan/PEG blended PLGA nanoparticle for tumor drug delivery. *Eur J Pharmacol* 670:372–383. doi:[10.1016/j.ejphar.2011.09.023](https://doi.org/10.1016/j.ejphar.2011.09.023)
- Prasad KN, Luong TT, Florence Joelle Paris AT, Vaution C, Seiller M, Puisieux F (1979) Surface activity and association of ABA polyoxyethylene–polyoxypropylene block copolymers in aqueous solution. *J Colloid Interf Sci* 69:225–232. doi:[10.1016/0021-9797\(79\)90151-6](https://doi.org/10.1016/0021-9797(79)90151-6)
- Shen M, Huang Y, Han L, Qin J, Fang X, Wang J, Yang V (2012) Multifunctional drug delivery system for targeting tumor and its acidic microenvironment. *J Control Release* 161:884–892. doi:[10.1016/j.jconrel.2012.05.013](https://doi.org/10.1016/j.jconrel.2012.05.013)
- Tian W, Chen Q, Yu C, Shen J (2003) Amino-terminated poly(ethylene glycol) as the initiator for the ring-opening polymerization of 3-methylmorpholine-2,5-dione. *Eup Polym J* 39:1935–1938. doi:[10.1016/S0014-3057\(03\)00091-0](https://doi.org/10.1016/S0014-3057(03)00091-0)
- Torchilin VP (2006) Multifunctional nanocarriers. *Adv Drug Deliver Rev* 58:1532–1555. doi:[10.1016/j.addr.2012.09.031](https://doi.org/10.1016/j.addr.2012.09.031)
- Vonarbourg A, Passirani C, Saulnier P, Benoit JP (2006) Parameters influencing the stealthiness of colloidal drug delivery systems. *Biomaterials* 27:4356–4373. doi:[10.1016/j.biomaterials.2006.03.039](https://doi.org/10.1016/j.biomaterials.2006.03.039)
- Wang Y, Yu L, Han L, Sha X, Fang X (2007) Difunctional pluronic copolymer micelles for paclitaxel delivery: synergistic effect of folate-mediated targeting and pluronic-mediated overcoming multidrug resistance in tumor cell lines. *Int J Pharm* 337:63–73. doi:[10.1016/j.ijpharm.2006.12.033](https://doi.org/10.1016/j.ijpharm.2006.12.033)
- Wang H, Zhao Y, Wu Y, Hu Y, Nan KH, Nie G, Chen H (2011) Enhanced anti-tumor efficacy by co-delivery of doxorubicin and paclitaxel with amphiphilic methoxy PEG–PLGA copolymer nanoparticles. *Biomaterials* 32:8281–8290. doi:[10.1016/j.biomaterials.2011.07.032](https://doi.org/10.1016/j.biomaterials.2011.07.032)
- Yadav AK, Mishra P, Mishra AK, Mishra P, Jain S, Agrawal GP (2007) Development and characterization of hyaluronic acid-anchored PLGA nanoparticulate carriers of doxorubicin. *Nanomed Nanotechnol* 3:246–257. doi:[10.1016/j.nano.2007.09.004](https://doi.org/10.1016/j.nano.2007.09.004)
- Yamamoto Y, Yasugi K, Harada A, Nagasaki Y, Kataoka K (2002) Temperature-related change in the properties relevant to drug delivery of poly-(ethylene glycol)-poly(L-lactide) block copolymer micelles in aqueous milieu. *J Control Release* 82:359–371. doi:[10.1016/S0168-3659\(02\)00147-5](https://doi.org/10.1016/S0168-3659(02)00147-5)
- Yang L, Wu XH, Liu F, Duan YR, Li SM (2009) Novel biodegradable polylactide/poly(ethylene glycol) micelles prepared by direct dissolution method for controlled delivery of anticancer drugs. *Pharm Res* 26:2332–2342. doi:[10.1007/s11095-009-9949-4](https://doi.org/10.1007/s11095-009-9949-4)
- Yoo H, Park T (2004) Folate receptor targeted biodegradable polymeric doxorubicin micelles. *J Control Release* 96:273–283. doi:[10.1016/j.jconrel.2004.02.003](https://doi.org/10.1016/j.jconrel.2004.02.003)
- Zelinskyy Y, May V (2011) Optical properties of supramolecular complexes coupled to a metal-nanoparticle: a computational study. *Chem Phys Lett* 511:372–377. doi:[10.1016/j.cplett.2011.06.066](https://doi.org/10.1016/j.cplett.2011.06.066)
- Zhang C, Ding Y, Yu LL, Ping Q (2007) Polymeric micelle systems of hydroxy-camptothecin based on amphiphilic *N*-alkyl-*N*-trimethyl chitosan derivatives. *Colloids Surf B* 55:192–199. doi:[10.1016/j.colsurfb.2006.11.031](https://doi.org/10.1016/j.colsurfb.2006.11.031)
- Zhao Y, Hua H, Chang M, Liu W, Zhao Y, Liu H (2010) Preparation and cytotoxic activity of hydroxycamptothecin nanosuspensions. *Int J Pharm* 392:64–71. doi:[10.1016/j.ijpharm.2010.03.027](https://doi.org/10.1016/j.ijpharm.2010.03.027)
- Zhao L, Zhu L, Liu F, Liu C, Shan D, Wang Q, Zhang C, Li J, Liu J, Qu X, Yang Z (2011) pH triggered injectable amphiphilic hydrogel containing doxorubicin and paclitaxel. *Int J Pharm* 410:83–91. doi:[10.1016/j.ijpharm.2011.03.034](https://doi.org/10.1016/j.ijpharm.2011.03.034)
- Zhao Y, Li J, Yu H, Wang G, Liu W (2012) Synthesis and characterization of a novel polydepsipeptide contained triblock copolymer (mPEG–PLLA–PMMD) as self-assembly micelle delivery system for paclitaxel. *Int J Pharm* 430:282–291. doi:[10.1016/j.ijpharm.2012.03.043](https://doi.org/10.1016/j.ijpharm.2012.03.043)
- Zhou Y, Du Y, Wang L, Yuan H, Zhou J, Hu F (2010) Preparation and pharmacodynamics of stearic acid and poly(lactic-co-glycolic acid) grafted chitosan oligosaccharide micelles for 10-hydroxycamptothecin. *Int J Pharm* 393:143–151. doi:[10.1016/j.ijpharm.2010.04.025](https://doi.org/10.1016/j.ijpharm.2010.04.025)